

# Wearable Sensor Node for Cardiac Ischemia Detection

Piotr Augustyniak

*AGH University of Science and Technology, Krakow, Poland*

**Keywords:** Wearable Sensor Network, Intelligent Sensors, Ischemia.

**Abstract:** Detection of cardiac ischemia based on early repolarization ECG markers has been widely recognized since three decades. It is also employed as a safety marker in exercise testing and cardiac rehabilitation. It assumes a standardized load applied to a patient in laboratory conditions, which diminishes patients' responsiveness and lowers the medical outcome statistics. A remedy consists in detecting ischemia markers during daily living activities in context of instantaneous physical load. Patients more willingly participate in diagnostics or rehabilitation, but the procedure requires specialized sensors and processors of ECG dedicated to use in domestic conditions. To this point we designed a small and lightweight autonomous two-lead ECG sensor node including heart rate and ST-segment processing algorithm and secure Bluetooth Low Energy connectivity to a supervising Wearable Sensor Network. In laboratory exercise tests with 50 ischemic patients the sensor issued alerts well coinciding with the output of a standard 12-lead system (with 2 fp and 1 fn cases). Moreover, in a two-lead setup the electrodes can be randomly applied to the skin in location best corresponding the ischemic region. Low power-oriented design and low transmission duty cycle result in continuous operation of the sensor for over a month with one coin battery.

## 1 INTRODUCTION

Recent developments of electronic and data communication technologies enable to build smart wearable devices for various medical purposes. This allows to shift several diagnostic or therapeutic procedures from hospitals to homes of patients increasing their comfort and responsiveness. Such intelligent sensors are organized in wireless sensor networks (WSN) applied directly on the human body (therefore called body sensor networks, BSN) or in the living premises creating active ecosystems for assisted living (e.g. Hao and Foster, 2008; Figueiredo et al., 2010; Sahoo et al., 2017). This idea has been applied far beyond the traditional areas of medical interest and helps children, elderly, danger-exposed professionals etc. to supervise their performance.

Coronary arteries provided the oxygenated blood to the heart muscle and cells of the conduction system, thus deficient oxygenation may result in arrhythmia, conduction blocks, ectopic beats or acute infarct and partial necrosis of the heart muscle. Two more facts should be noted here: (1) although ground-truth ischemia markers require biochemical blood analysis, its influence to the early

repolarization stage allow for reliable detection based on ST segment in the electrocardiogram (O'Gara et al., 2013) and (2) in most cases ischemia is localized in heart muscle regions depending on the topology of inefficient coronary vessels. Therefore in a regular 12-lead exercise system, in one person the ST-segment changes dominate in V1, V2 and in another person in V5, V6 precordial leads depending on localization of atherosclerosis (Menown et al., 2000).

The need for reliable instrumentation for a daily life condition exercise test or cardiac rehabilitation motivated us to design an autonomous ischemia sensor cooperating as a node of WSN with accelerometers, posture and pressure sensors estimating the physical load. The network is supervised by a wearable server accompanying the patient during the outdoor activity or by a stand-alone hub embedded to the infrastructure of the patient premise (e.g. dormitory). An example of universal wearable biosignal recorder with a Bluetooth-extensible WSN was presented in our previous paper (Augustyniak, 2016), but the ischemia detector is expected to work correctly with any device (e.g. a smartphone) with complying communication protocol.

Usually ischemia alerts are defined as ST-segment amplitude crossing of arbitrarily given thresholds, and therefore criticized for their dependence on subject fitness. Due to the poorer propagation of heart-related electrical phenomena to the body surface, obese people in general show lower ECG amplitudes and the ischemia signs are underrepresented in amplitude measurements of ST-segment. The other concern is the adjustment of the ST-segment length with heart rate changes. In exercise and daily living ECG recordings the heart rate varies from 50 to 180 in healthy adults, so various correction methods are implemented in the interpretive software. Bazett formula (Bazett, 1920) is one of most frequently referred, but some cardiologist believe it is not equally suitable for all subjects. Accordingly to the paradigm of personalized medicine our ischemia sensor allows for parametrization of several on-board signal processing factors (e.g. threshold values or correction method) by a supervising device through the wireless communication channel.

## 2 IMPLEMENTATION DETAILS

The prototype wearable sensor node for ischemia detection was designed and build for exploration of new diagnostic purposes and usage scenarios it may offer for cardiology. This paper presents the prototype, while industrial research are continued on the target circuitry, processing platform and form factor. The prototype was designed as an autonomous device identified by a supervising device and working as a node of sensor network. This device has not been presented in this paper, we simply assume that it uses a compatible Bluetooth Low Energy (BLE) protocol, is able to identify, initialize and query the node and collects the received data packets. The supervising device may be wearable or stationary and may equally manage other sensors within the network.

The design of prototype ischemia detector needed will be presented in subsequent sections in three main engineering aspects: the recording and processing hardware, the processing algorithm and the communication module.

### 2.1 Recording and Processing Hardware

We based on experience gathered in our previous project on wearable wireless heart rate monitor for continuous long-term variability studies

(Augustyniak, 2011). The prototype wearable monitoring device (fig. 1) is designed as lightweight (7.3 g) and reduced in size (below 1 sq inch). With these physical properties the device It is based on the ARM7 family processor (Atmel AT91SAM7X256), running at 18 MHz due to very low power consumption (0.5 mW). It is powered by a replaceable 3.0 V Li-Manganese Dioxide coin battery (CR2032, 220 mAh, diameter 20 mm, weight 2.5 g) allowing for 940 hours (i.e. 39 days) of continuous work. A single-channel low-power (0.2 mW) analog front-end was custom-built and verified for compliance with a typical ECG measurement specification (full range  $\pm 12$  mV, noise  $1\mu\text{V RMS}$ ,  $k_u = 85\text{V/V}$ ). Further reduction of the footprint and the power consumption down to  $0.2\mu\text{W}$  is possible with the use of custom-designed analog or mixed-signal chip manufactured in  $0.18 - 0.35\mu\text{m}$  CMOS technology (Liu et al., 2010; Tseng et al., 2012; Teng et al., 2014). These options are considered for further development of the prototype to a commercial product. Besides the battery life, the limitation of long time electrophysiological recordings is the stability of skin-electrode contact, which currently allows for two weeks continuous data capture (Weder et al., 2015). Alternative approaches use capacitive coupling for ECG recording (Ueno et al, 2007), but for maintaining low frequency throughput required for ST-segment diagnostics large electrode size is required.

The ECG is acquired with the processor built-in sigma/delta analog to digital converter at a sampling frequency of 1000 sps and 16 bits resolution. a short buffer of memory stores approximately 4 seconds of signal in case of the algorithm requires reprocessing the raw signal (e.g. search back procedure when no heart beat detected for more than 2 s.). In a service mode, the prototype enables a direct digital input data stream and yields the raw digital ECG signal at internal connector pins. Otherwise, the recorded ECG is abandoned once the ST-segment calculations are completed.

We tried to minimize the size of the prototype to test its properties as a device worn at everyday living activities. Twin printed circuit boards with analog and digital circuitry include the battery and the BLE antenna. One electrode snap is directly embedded into the board and, besides the electric contact, used to hold the device attached to the skin, while the other is mounted at the end of a 12 cm wire (fig. 1).



Figure 1: Circuitry of a prototype wearable sensor for ischemia detection.

## 2.2 Processing Algorithm

The ECG processing algorithm works in real time regime. A regular delay between the QRS occurrence and the availability of heart beat description is 1.6 s and can occasionally be extended to 3.6 s in case of search back for a missed heartbeat.

The ECG waveform needs a specific processing to yield the annotated heart beats positions and ST-segment description (fig. 2). Single-lead electrocardiogram is sufficient to provide reliable temporal markers and thorough information about the origin for each heartbeat. Since ectopic beats propagate through alternative conduction pathway, only sinoatrial beats are considered for detection of ST-segment-based ischemia markers. The processing algorithm consists of QRS detection, morphology detection and ST-segment processing procedures presented in subsequent sections.

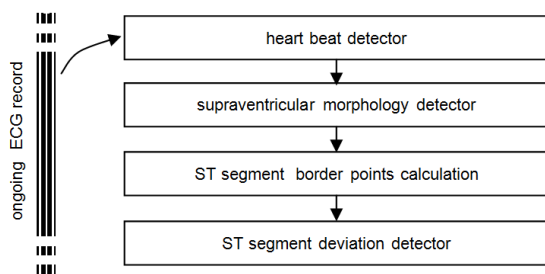


Figure 2: Block diagram of on-board processing software for ischemia detection.

### 2.2.1 Heartbeat Detection

Although the ECG is acquired with 1ksps, a subsampled (decimated) version of 250 sps is used

for heart beat detection in real time. This procedure first calculates a detection function with the use of signal filtering and mathematical transformations favouring the features common for the QRS complex accordingly to a modified Pan-Tompkins algorithm (Pan and Tompkins, 1985). Although long filter buffers result in significant delay in QRS detection, we prefer this classical approach for its very low computational complexity.

Next, an adaptive threshold is applied to determine the rough position of each QRS section. In case no QRS is detected in more than 2 s (i.e. 500 samples) a search-back procedure is employed to scan again the detection function with a lower threshold value. The search back helps finding small supraventricular beats following a pair or series of high ectopic beats.

The precise localization of the R wave peak is further refined to 1 ms with the use of five points-based parabola fitting (Augustyniak, 1999). Since main QRS components fall far below 125 Hz, this approach is more robust to the noise and determines the QRS more precisely than a direct Pan-Tompkins algorithm applied to a 1ksps ECG time series. Additionally, the average difference between the parabola samples and corresponding ECG samples is taken as a measure of recorded noise. Excess of a programmed noise threshold activates the noise flag and deactivates other ST-segment-related alerts as unreliable.

### 2.2.2 Morphology Detection

The on-board ECG morphology detection is restricted to the set of features necessary for supraventricular beats identification (de Chazal et al., 2004). The classification procedure distinguishes normal sinus beats (N) from arrhythmic beats (V, others, artefacts) and, following the power economy, is organized in two stages.

First, the rhythm stability is assessed by beat-to-beat comparison of two features: the difference of signal sections isolated in the  $\pm 100$  ms (i.e. 200 samples) vicinity of consecutive R wave peak and the difference of RR-interval. Next, if both values fall below the respective thresholds, the beat origin attribute is copied from the precedent beat. Large differences in beat shapes or RR intervals indicate the possible occurrence of other morphologies that need to be excluded from ST-segment analysis. The value of threshold is initially set to 10% but may be modified in sensor initialization stage.

Only for beats with over threshold difference, signal-based geometrical features selected as the

most discriminative for atrial and ventricular beats (the surface to perimeter ratio and the count of samples of over-threshold speed) are calculated and contribute to the final decision about the beat origin attribute (Augustyniak, 1997). The morphology detector is tuned to restrictively eliminate abnormal heartbeats (prefers false negative cases). Erroneous inclusion of a single ectopic beat leads to false ST-segment measurements and probable false ischemia alerts. Erroneous exclusion of a true sinus beat, if occurs occasionally, is delaying but not otherwise influencing the ischemia detection.

### 2.2.3 ST-segment Processing

The ST segment is identified as following the R wave by 60 ms (J-point) and lasting for 80 ms at a heart rate of 60 beats per minute (Jensen et al., 2005). As the duration of repolarization phase varies with the hearth rhythm change, several mathematical formulas (known as Bazett, Fredericia, Framingham and Hodges) have been proposed for correction of QT interval length (Funck-Brentano and Jaillon, 1993). Since the ST-segment is a part of QT interval, the correction is also applicable for determining ST-segment border points at which amplitudes are measured and taken as ischemia markers. All above correction formulas were implemented in the on-board software of ischemia sensor. Two configuration bytes are used for correction management: one defines the R-to-J distance (fig. 3) and the other selects the length correction method.

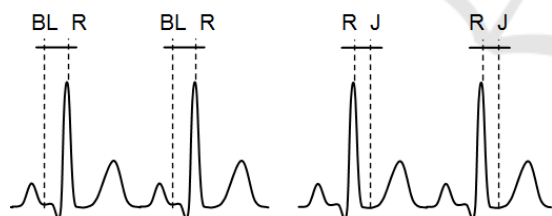


Figure 3: Definitions of baseline (BL) and ST-segment beginning (J) points for amplitude measurement used in ischemia markers detection.

Two variables are calculated on ST-segment: the elevation/depression and the slope. Flat, downsloping, or depressed ST segment may indicate coronary ischemia. ST elevation may indicate transmural myocardial infarction, while ST depression may be associated with subendocardial myocardial infarction or other serious heart failures.

The ST elevation/depression is measured as difference of average values of ECG signal samples between ST-segment border points and average values of ECG signal samples on baseline preceding

the QRS complex. The positive value of difference is called ‘elevation’, while the negative is called ‘depression’.

The ST-segment slope is measured as the slope coefficient of the straight line best fitted to ECG signal samples between ST-segment border points (fig. 4). The slope can be either positive (upwards) or negative (downwards).

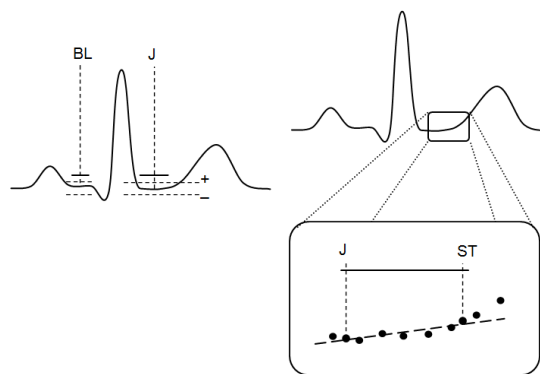


Figure 4: Definitions of ischemia markers: a) elevation/depression, b) slope.

Although the adopted definitions originate from medical recommendations, we cannot implement a single borderline value between normal and abnormal results as it is common in 12-lead exercise ECG systems (usually 100  $\mu$ V for ST elevation). In a single-lead ischemia sensor with not defined electrode positions, the threshold values for ST-segment elevation and slopes are then programmed at the configuration stage. Depending on electrode position the elevation may turn to depression and the slope direction may change (Jiang et al., 2009).

## 2.3 Communication Module

The ischemia sensor is dedicated to work as a slave device in a BSN organized with Bluetooth Low Energy (4.0) technology using either a peer-to-peer connection, either a star topology. The supervising device initializes, controls and reads all sensors in the network accordingly to the programmed schedule or to the occurrence of ST events.

The communication begins with short data packets allowing to identify and initialize the sensor and establish a short time secure channel to transmit the configuration and long term key. The initialization procedure is performed repeatedly for verification of the sensor status (e.g. battery level), time synchronization or key update. Connection setup and data transfer are completed within 3 ms, allowing the supervising device to check and

synchronize the ischemia sensor in short time and at a cost of very low energy.

In a typical exercise test ST-segment properties change in response to the physical load thus the output data are transmitted in synchronous packets at the end of programmed reporting interval (1 – 256 s) or asynchronously at each heartbeat interval. The continuous mode or immediate reporting is not economical, but exercise test are usually performed in laboratory condition and last for 30 minutes.

In a typical rehabilitation or surveillance scenario, a heartbeat interval (RR) should be kept within a specified range. Excess of the RR range borders or ST elevation/depression measure is detected by on-board software and triggers occasional asynchronous reporting. In this mode connection duty cycle is very low improving data security and power saving. This is particularly useful for everyday living conditions.

The configuration packet has a length of 32 bytes consists of:

- two configuration bytes for heartbeat and morphology detectors,
- two configuration bytes for ST-segment alignment and length correction,
- four bytes of HR and ST thresholds setup,
- two bytes for reporting mode setup,
- twenty bytes of long term security key.
- two spare bytes for further sensor configuration.

The report packet has a length of 8 bytes and consists of:

- two bytes of sensor status report,
- four bytes of diagnostic data: RR-interval, ST-segment elevation and slope,
- one byte of actual ST segment length,
- one byte of threshold excess flags.

The BLE uses modern communication technology and security-oriented transmission protocols. The security of low-energy transmission within the BSN is based on AES-CCM encryption algorithm with exclusive long time keys passed from supervising device to each remote sensor via individual temporary secure channels. A short term key for the temporary channel is a string of 6 numeric digits generated uniquely for each pairing (Padgette et al., 2017). Since the sensor configuration session occurs randomly and lasts for only few milliseconds, the man-in-the-middle attacks have little chance to success.

### 3 EXPERIMENTAL VALIDATION

#### 3.1 Testing Conditions

The prototype was tested in three laboratory conditions (referred to by their numbers):

1. with arbitrary waveform generator replaying the pre-recorded real exercise ECG of known HR and ST-segment results,
2. with cardiac patients undergoing a regular stress test diagnosis for possible cardiac ischemia as accompanying device,
3. with three human volunteers performing everyday living activities including physical training (jogging) or work (gardening).

In all experiments the sensor was supervised by a smartphone with purpose-built application in peer-to-peer mode. In experiment 2 the smartphone clock was synchronized with the exercise test system. Sensor-originated medical measurements were stored in the smartphone memory (microSD card) for further analysis.

Experiment 1 was performed with 30 half-hour records made with commercial stress test system (by Aspel) during a Bruce protocol treadmill test (Bruce, 1974). Recorded full disclosure 12-lead electrocardiograms were first replayed digitally to validate the correctness of sensor on-board ECG interpretation procedures (fig. 2). Once the validation was successful, we replayed the signals again through the digital to analog converter and fed to the bipolar inputs of the sensor in three various combinations: V1-V3, V4-V6 and V2-V5. Consequently, we had 90 half hour test signals with reference.

Experiment 2 was performed during 20 regular half-hour stress test diagnoses in patients suspected for possible cardiac ischemia. Diagnostic records were made with commercial stress test system during a Bruce protocol treadmill test. The electrodes of the tested prototype were placed in two irregular locations orthogonal to the chest leads line: symmetrically 5 cm over and under V2 and symmetrically 5 cm over and under V5 lead. In this experiment we tested the difference of ischemia detection between the proposed wearable sensor and the commercial exercise system.

Experiment 3 was performed in three young volunteers wearing the sensor for 72h each during everyday living activities including physical training (jogging) or work (gardening). The recorded time series of HR and ST measurements were compared

to the activity record manually made by the subject. The alert threshold HR was set to 110 bpm, and amplitude to 50  $\mu\text{V}$  in order to detect exercise induced ischemia markers in healthy people.

### 3.2 Testing Results

Values of medical measurements HR and ST calculated by the sensor in Experiment 1 were compared to the annotations made by medical staff on a source 12-lead exercise record. The setup used raw ECG signals pre-recorded with 12-lead system, thus it simulated electrode placement in exact positions of V1-V3, V4-V6 and V2-V5 respectively. Consequently in each configuration, the results from the sensor were referred to the respective ECG channels (tab. 1).

Table 1: Results of Experiment 1 – comparing HR and ST calculated by the sensor to the annotations made by medical staff on a source 12-lead exercise record.

Parameter	Value
Amplitude measurement accuracy	1.5 $\mu\text{V}$ (5 LSB)
Average HR difference	0.7 bpm
Standard deviation of HR	1.7 bpm
Average difference of ST elevation/depression	5.0 $\mu\text{V}$ (16 LSB)
Standard deviation of difference of ST elevation/depression	8.2 $\mu\text{V}$ (27 LSB)
Average difference of ST slope coefficient	0,03 $\mu\text{V/s}$
Standard deviation of ST slope coefficient	0,12 $\mu\text{V/s}$

In experiment 2 the sensor was used simultaneously to commercial exercise test system during 20 regular half-hour stress test diagnoses. In eight out of the 20 patients cardiac ischemia was diagnosed based on the outcome of the commercial system. The sensor electrodes were positioned in alternative location to the 12-lead system, thus direct comparison of amplitudes were not possible. Consequently, with ST alert threshold set to 100  $\mu\text{V}$ , we investigated false detection cases and temporal difference of ischemia detection between the sensor and the commercial system (tab. 2).

Table 2: False detection and temporal difference of ischemia detection analysis.

Parameter	Value
Threshold excess time difference	8 s
Standard deviation of threshold excess time	17 s
False positive ischemia detection	2
False negative ischemia detection	1
True positive ischemia detection	47
True negative ischemia detection	20

In experiment 3 the sensor was used in three healthy volunteers with no previous ischemia record to detect the physical exercise events of two types (jogging and gardening) in their everyday life. As the exercise manifests itself in slight deviations of ST-segment measurements, we programmed lower values of alert thresholds (110 bpm for HR and 50  $\mu\text{V}$  for ST elevation). The sensor electrodes were positioned at V2-V5 location. The sensor was paired with a smartphone and the subjects were asked to always recharge the battery at night (i.e. where no activity is performed) in order to capture all exercise-related ST events. During a continuous 72 hour session the subjects were asked to act accordingly to their regular activity with taking notes on beginning and ending time (tab. 3).

Table 3: Statistics of physical activity detected by the sensor and reported by the volunteers.

Parameter	Value
Jogging events	7
Average jogging events duration	41 ( $\pm$ 17) min
Jogging start to HR threshold excess time (average $\pm$ STD)	45 ( $\pm$ 18) s
Jogging start to ST elevation threshold excess time (average $\pm$ STD)	170 ( $\pm$ 51) s
Gardening events (digging)	19
Average gardening events duration	3.3 ( $\pm$ 4.1) min
Gardening start to HR threshold excess time (average $\pm$ STD)	27 ( $\pm$ 37) s
Gardening start to ST elevation threshold excess time (average $\pm$ STD)	71 ( $\pm$ 54) s

## 4 DISCUSSION

A small and lightweight intelligent sensor for ischemia detection has been proposed, designed and prototyped.

First tests with pre-recorded signals helped to evaluate the correctness of on-board software implementation and accuracy of performed measurements. A detailed review of errors leads to the conclusion that amplitude measurements accuracy is of order of 5 LSB (1.5  $\mu\text{V}$ ), and values of ST segment amplitude-related errors greater than that are due to occasional false positive or false negative morphology detection. Nevertheless, in comparison with regular 12-lead exercise test systems the measurement accuracy of the ischemia sensor is competitive. The accuracy of ST slope coefficient cannot be quantitatively compared, since no known exercise test system provide respective technical data. Most systems simply state the slope is going upward (positive coefficient) or downward (negative coefficient), what is sufficient for medical purposes.

In Experiment 2 the sensor was tested simultaneously to a commercial exercise test system with several patients, in some of which cardiac ischemia was diagnosed. Although the wearable sensor used alternative lead positions, the test proved acceptable detection accuracy and reasonable simultaneity of detection. The true accuracy of ECG exercise stress testing for ischemia detection is only of about 75% and all ambiguous cases are subject to further diagnostics based on coronary catheterization or magnetic resonance imaging. Since no such verification was made in our case, the false detection cases may be interpreted in reference to a commercial stress test system, and not in reference to a ground-truth medical diagnosis of cardiac ischemia.

Third experiment showed that the cardiac ischemia sensor is a truly wearable device, even if the prototype is too large and cumbersome for unobtrusive operation in daily living conditions. The accurate detection of physical load with the heart rate is not surprising, but, what is more relevant in our case, can also be reliably done with change of ST parameters. What is most important in our case, the ST segment changes may be analysed in context of the heart rate, what enabled detection of ECG ischemia markers during random physical activity taken by the subject. Moreover, during this test the sensor worked in asynchronous reporting mode, where the excess of the RR or ST elevation/depression range borders is detected by

on-board software and triggers occasional reporting. Average power consumption with twelve short communication sessions a day was estimated to 0.8 mW, what grants a month of autonomous operation without battery replacement.

The presented study has several limitations: only one prototype was build, simplified algorithms were used for heart beats detection and morphology classification, the number of patients was small, and the number of those with ischemia was even smaller. Therefore, we consider our work as a proof of concept and are looking forward to build an industrial prototype and test it in clinics with true ischemia reference. This would reveal one of the expected advantage of the sensor which consists in unrestricted electrode positions.

The performance of proposed wearable system is comparable to a standard 12-lead exercise test system. Thanks to reduced weight and size and prolonged autonomy its application area extends to everyday activity detection and risk stratification in home monitoring. With a wearable ischemia sensor, the cardiologists may extend the scope of their cardiac surveillance get better responsiveness from their patients and optimize the monitoring accordingly to patients' medical history (e.g. localization of the infarct).

## ACKNOWLEDGEMENTS

This work is supported by the National Centre for Research and Development (NCBiR) under Grant No. STRATEGMED/269043/20/NCBR/2017

## REFERENCES

- Augustyniak, P., 1997. The use of shape factors for heart beats classification in Holter recordings. In *Computers in Medicine Conf.* pp. 47-52.
- Augustyniak, P., 1999. Recovering the precise heart rate from sparsely sampled electrocardiograms. In *Computers in Medicine Conf.* pp. 59-65.
- Augustyniak, P., 2011. Wearable wireless heart rate monitor for continuous long-term variability studies. *Journal of Electrocardiology*, vol. 44 no. 2 pp. 195–200.
- Augustyniak, P., 2016. Remotely Programmable Architecture of a Multi-Purpose Physiological Recorder", *Microprocessors and Microsystems* vol. 46 pp. 55-66 DOI: 10.1016/j.micpro.2016.07.007.
- Bazett, J. C., 1920. An analysis of time relation of electrocardiograms. *Heart* vol. 7, pp. 353–367.

- Bruce, R. A., 1974. Methods of exercise testing: Step test, bicycle, treadmill, isometrics. *Am. J. Cardiol.* vol. 33, iss. 6, pp. 715-720.
- de Chazal, P. D., O'Dwyer, M., Reilly, R. B., 2004. Automatic classification of heartbeats using ECG morphology and heartbeat interval features. *IEEE Trans. on Biomedical Engineering*, vol. 51, pp. 1196-1206.
- Figueiredo, C. P., Becher, K., Hoffmann, K. P., Mendes, P.M., 2010. Low power wireless acquisition module for wearable health monitoring systems. In *32nd IEEE EMBS Conf. 2010*, pp. 704-707.
- Funck-Brentano, C., Jaillon, P., 1993. Rate-corrected QT interval: techniques and limitations. *Am J Cardiol.* 72(6):17B-22B.
- Hao, Y., Foster, R., 2008. Wireless body sensor networks for health monitoring applications. *Physiological Measurement*, vol. 29, R27.
- Jensen, B. T., Abildstrom, S. Z., Larroude, C. E., Agner, E., Torp-Pedersen, C., Nyvad, O., Ottesen, M., Wachtell, K., Kanters, J. K., 2005. QT dynamics in risk stratification after myocardial infarction. *Heart Rhythm.* vol. 2 no. 4, pp. 357-64. DOI:10.1016/j.hrthm.2004.12.028.
- Jiang, Y., Qian, C., Hanna, R., Farina D., Doessel, O., 2009. Optimization of electrode positions of a wearable ECG monitoring system for efficient and effective detection of acute myocardial infarction, In *36th Annual Computers in Cardiology Conference (CinC)*, pp. 293-296.
- Liu, X., Zheng, Y. J., Phyu, M. W., Zhao, B., Je, M., Yuan, X. J., 2010. A miniature on-chip multi-functional ECG signal processor with 30  $\mu$ W ultra-low power consumption. In *32nd IEEE EMBS Conf 2010*, pp. 2577-2580.
- Menown, I. B., Mackenzie, G., Adgey, A. A., 2000. Optimizing the initial 12-lead electrocardiographic diagnosis of acute myocardial infarction. *European Heart Journal*, vol. 21, no. 4, pp. 275-83.
- Moyer, V. A., 2012. Screening for coronary heart disease with electrocardiography: US Preventive Services Task Force recommendation statement. *Annals of Internal Medicine*, vol. 157, pp. 512-518.
- O'Gara, P. T. et al., 2013. 2013 ACCF/AHA Guideline for the Management of ST-Elevation Myocardial Infarction. *Circulation.* vol.127, pp. e362-e425.
- Padgett, J., Scarfone, K., Chen, L., 2017. 2017 Security Guide to Bluetooth - Recommendations of the National Institute of Standards and Technology, Special Publication 800-121 Revision 2, [Online] <http://nvlpubs.nist.gov/nistpubs/SpecialPublications/NIST.SP.800-121r2.pdf> (accessed 30.06.17).
- Pan, J., Tompkins, W. J., 1985. A real-time QRS detection algorithm. *IEEE Transactions on Biomedical Engineering*, vol. 32, no. 3, pp. 230-236.
- Ueno, A., Akabane, Y., Kato, T., Hoshino, H., Kataoka, S., Ishiyama Y., 2007. Capacitive Sensing of electrocardiographic Potential Through Cloth From the Dorsal Surface of the Body in a Supine Position: A Preliminary Study. *IEEE Transactions on Biomedical Engineering*, vol. 54, no. 4, pp. 759-766.
- Walsh, J. A., Topol, E. J., Steinhubl, S. R., 2014. Novel Wireless Devices for Cardiac Monitoring. *Circulation*, vol. 130, no. 7, pp. 573-581. <http://doi.org/10.1161/CIRCULATIONAHA.114.009024>.
- Weder, M., Hegemann, D., Amberg, M., Hess, M., Boesel, L. F., Abächerli, R., Rossi, R. M., 2015. Embroidered Electrode with Silver/Titanium Coating for Long-Term ECG Monitoring. *Sensors* (Basel, Switzerland), vol. 15, no. 1, pp. 1750-1759. <http://doi.org/10.3390/s150101750>.
- Sahoo, P. K., Thakkar, H. K., Lee, M.-Y., 2017. A Cardiac Early Warning System with Multi Channel SCG and ECG Monitoring for Mobile Health. *Sensors*, vol. 17, 711; doi:10.3390/s17040711.
- Teng, S-L., Rieger, R., Lin, Y-B., 2014. Programmable ExG Biopotential Front-End IC for Wearable Applications, *IEEE Transactions on Biomedical Circuits and Systems.* vol. 8 no. 4, pp. 543-551.
- Tseng, Y., Ho, Y., Kao, S., Su, C., 2012. A 0.09  $\mu$ W Low Power Front-End Biopotential Amplifier for Biosignal Recording, *IEEE Transactions on Biomedical Circuits and Systems.* vol. 6, no. 5, pp. 508-516.